# Building Reconstruction from Synthetic Aperture Radar Images and Interferometry

Franz W. Leberl, Regine Bolter
*Institute for Computer Vision and Graphics*
*Graz University of Technology, Inffeldgasse 16, A-8010 Graz, Austria, leberl@icg.tu-graz.ac.at*

ABSTRACT: Imaging radar has recently become available at geometric resolutions high enough to begin thinking about mapping of individual buildings with their 3-dimensional shapes. This is based on interferometric elevation data as well as magnitude images with their shadows and layover representations from vertical objects. We discuss how an automated procedure can build models of buildings at an accuracy of ± 1 meter, given radar images with pixel diameters of 30 cms.

## 1. HIGH RESOLUTION RADAR IMAGES

### 1.1 *Geometric Resolution at 30 cms*

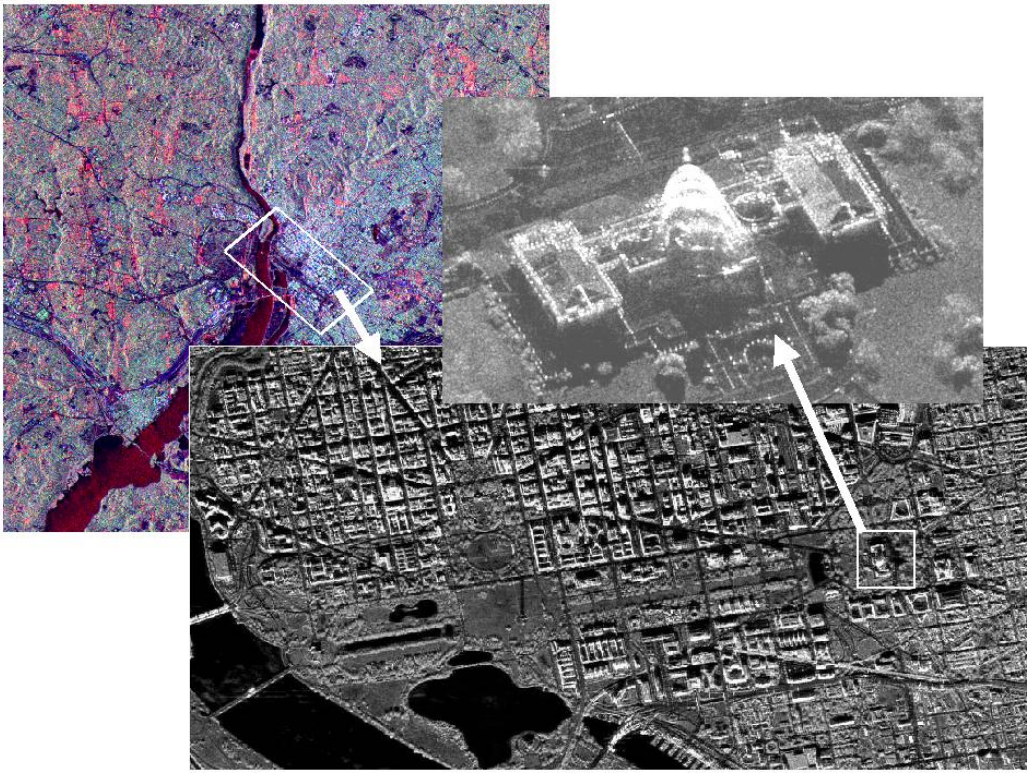

Figure 1: The same area shown at three different SAR resolutions, namely a temporal ERS-1 scene on the upper left, an airborne scene on the lower right and the full resolution of the airborne sensor on the upper right. Note Washington's Capitol building with the detail of the roof and vegetation at 30 cm pixel size (Courtesy esa, Sandia).

Current high-resolution airborne radar images are being produced at pixel sizes of perhaps 30 cm. This contrasts with previous values at 2.5 m, for example in the commercial system Star-3 of Intermap Technologies (Wang et al. 2001). From satellites, this resolution is currently at 6 m from Radarsat-1, and will improve to 3 m in the upcoming Radarsat-2. The European Terrasat proposal plans on a satellite SAR at 1 m pixel size. Examples of sub-meter resolution images can be found on the Internet under www.sandia.gov and an example is shown in Figure 1. We have selected such images for studies on fully automated building reconstruction. A SAR image example is presented in Figure 2. For comparison, Figure 3 presents the aerial photograph of the same site. Such images are the basis for studies to map buildings (Burkhart et al. 1996; Gamba et al. 2000; Hoepfner et al. 1998, Xiao et al. 1998).

Figure 2: Synthetic Aperture Radar (SAR) test data set of a few rural buildings at a resolution of 30 cm per pixel and imaged from the 4 cardinal directions. The area covers approximately 220 x 220 m². The images are presented with the flight line always from left to right on top (Courtesy Sandia).

Figure 3: Aerial photograph of the test site shown in Figure 2. The area covers approx. 220 x 220 m².

## 1.2 *Interferometry*

The most exciting innovation in the imaging radar area is interferometry. The original 1960's approach to interferometry was with optical processors and resulted in rather crude results. Since the later half of the 1980's, interferometry is available in digital form. The earliest such data were probably those obtained from two passes of the SEASAT satellite, flown in 1978. The most recent decennium has seen various new SAR-system developments with interferometric components. Figure 4 is the interferometric data set associated with the images in Figure 2. It is to be noted that it is customary to present such data in the form of so-called "ground ranges". This requires that the radar's range and interferometric angle measurement be used to transform the natural slant ranges into a form of an ortho-photo. However, the noise in the elevations tends to destroy the fine linear detail in the images so that sharp edges get "fuzzied up".

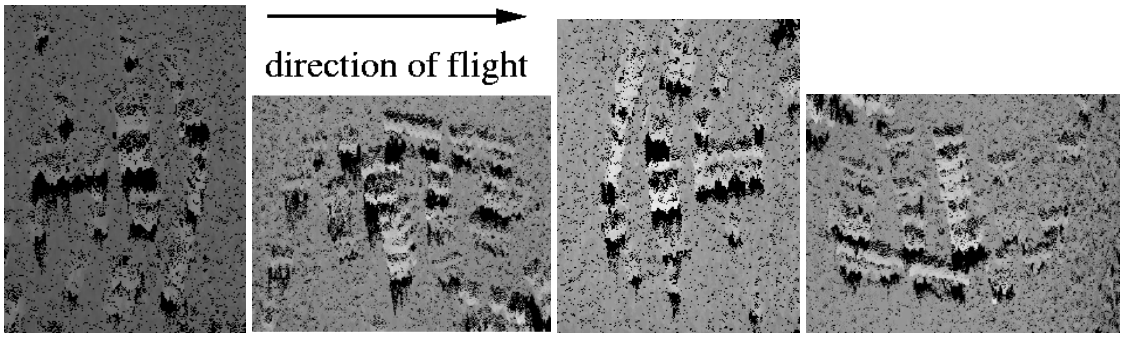


Figure 4: Interferometric data for the SAR images in Figure 2. The noisy appearance of the data is the result of the ground range presentation of the data using the noisy elevations obtained from interferometry. The area covers approx. 220 x 180 m² (Courtesy Sandia).

## 2 AUTOMATED PROCEDURE OF BUILDING RECONSTRUCTION

The task exists to design an automated procedure to map the 3-dimensional shape of buildings from the SAR images and interferometric point clouds. Figure 5 summarizes the approach. In the first stage slant range and ground range data are exploited separately. Combining multiple view interferometric height data elevated objects are extracted and together with the corresponding coherency information natural and man-made objects are separated (Bolter & Leberl 2000d). On the other hand from the slant range SAR magnitude images shadow areas are segmented and the resulting building's outlines from multiple views are grouped (Bolter & Leberl 2000b).

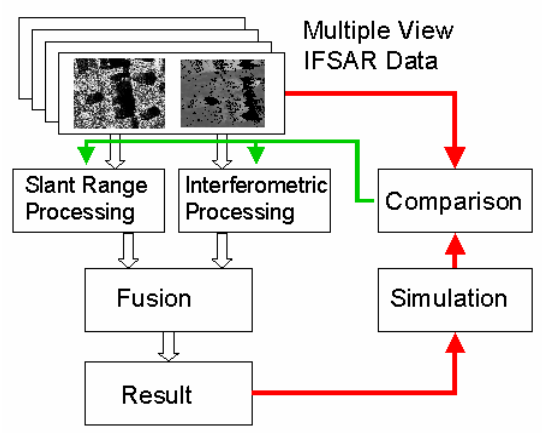


Figure 5: Procedure for the extraction of building models from a combination of SAR images and associated interferometric data (Bolter 2001).

In the second stage the outcome from the slant range processing and the exploitation of the interferometric SAR data are fused (Bolter & Leberl 2000c). The result is an initial coarse model of the scene. This resulting scene model is then used as input DEM into a simulator (Bolter 2000, Bolter & Leberl 2000a), the resulting simulated data are compared to the real data. Remaining differences between real and simulated data can be identified and used to refine the model in a second processing pass (Bolter & Leberl 2000e). This feedback process could be continued until the model is sufficiently accurate or until no further refinements are possible.

## 3 SIMULATIONS

A key tool in the research work for building modeling from SAR is a simulation system. Burkhart et al.(1996) was able to explain the so-called "front porch" effect in SAR interferometry with the help of simulation. Figure 6 illustrates the help one can get from simulation: the SAR views of one building in Figure 2 can be better interpreted with the help of a simulation. The phenomena of shadows, lay-overs, multiple reflections become better described in a simulation and can be identified in a real image based on a simulation.

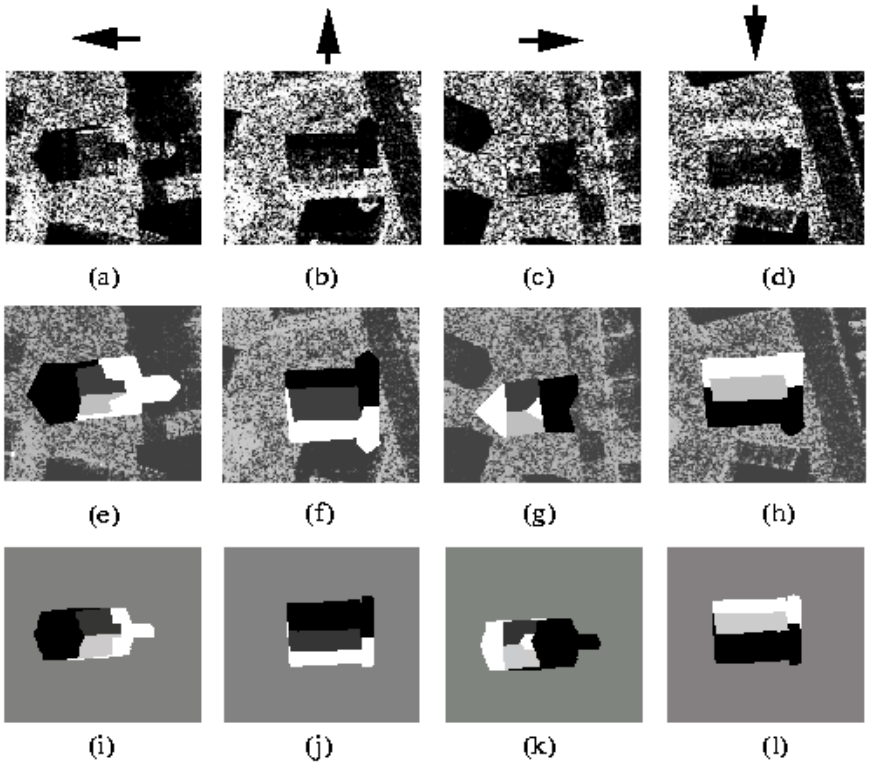


Figure 6: Four rectangular views (a) - (d) of the church in the test scene (Fig. 2) with the arrows indicating the flight directions. Real images are compared to simulated data using the model of the church (i) - (l). The radiometric differences in the simulated images are enhanced to study the phenomena which occur. Black regions are shadow regions, white areas correspond to layover and the two different gray regions correspond to the front and back part of the roof. From these simulated data it is possible to identify the same phenomena in the real data, they were identified manually in (e)-(h) . The area covers approx. 40 x 50 m².

Figures 7a, c, d present 3 views of the buildings in the test area, each made with a different scale for the vertical coordinate of the buildings. As the buildings get taller, their images begin to interact more with one another. Shadows begin to fall on top of layovers and reflections from adjacent buildings, the interpretation of such SAR images is getting more difficult. The interferometry (Fig. 7b) suffers from an increasing influence of the so-called “front-porch” effect, the interferometric version of the radar layover.

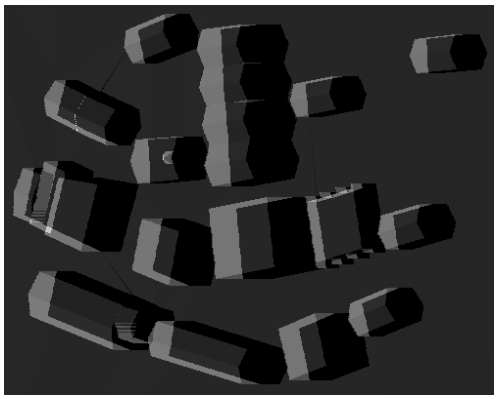

(a) Simulated slant range SAR image using true buildings heights between 5m and 15 m.

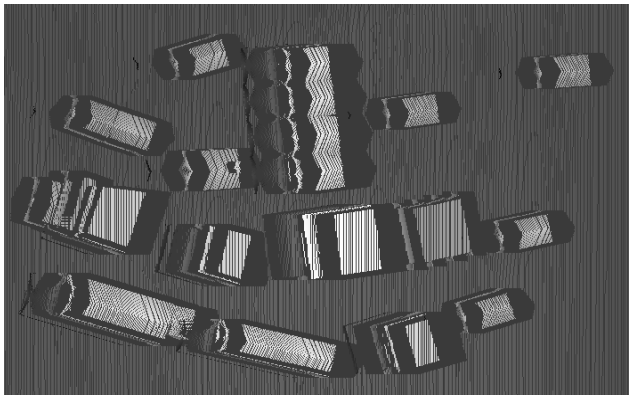

(b) Simulated ground range interferometric height data using true building heights.

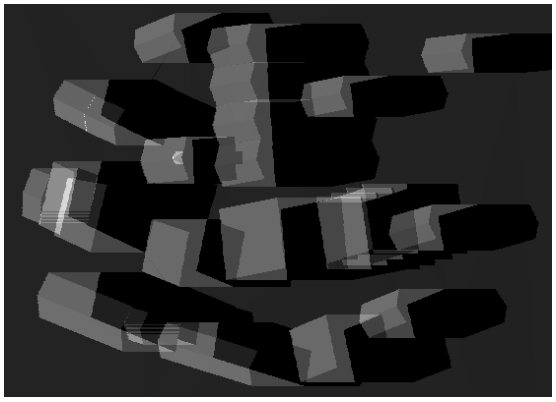

(c) Simulated slant range SAR image with all building heights increased by 15m.

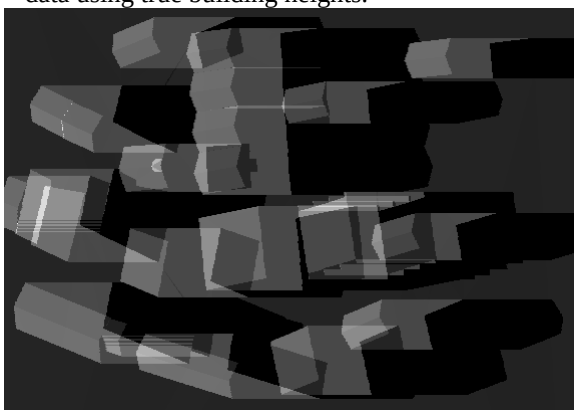

(d) Simulated slant range SAR image with all building heights increased by 30m.

Figure 7: Three slant range SAR image simulations of the same buildings, assuming three different building heights (a), (c) and (d). The simulated interferometric height data (b) in ground range projection correspond to (a). The area covers approximately 220 x 220 m².

## 4 ANALYSIS OF INTERFEROMETRIC POINT CLOUDS

The procedure to extract buildings from the interferometric data alone operates as follows:

superimposing the individual interferometric data sets from separate flights;
assigning to each pixel a single elevation based on the multiple elevation data from the multiple interferometric flights;
using a minimum filter to find the “bald Earth”;
separating the vertical objects from the bald Earth;
separating candidate pixels for buildings from non-buildings using the interferometric coherence data;
fitting sample building shapes to the remaining pixel concentrations indicative of buildings.

This approach is modeled after the work performed by Xiao et al. (1998). Figure 8 shows the result of this procedure applied to the multiple view simulated interferometric height data of the test scene assuming three different building heights (Fig. 8a-c) compared to the result from real data (Fig. 8d).

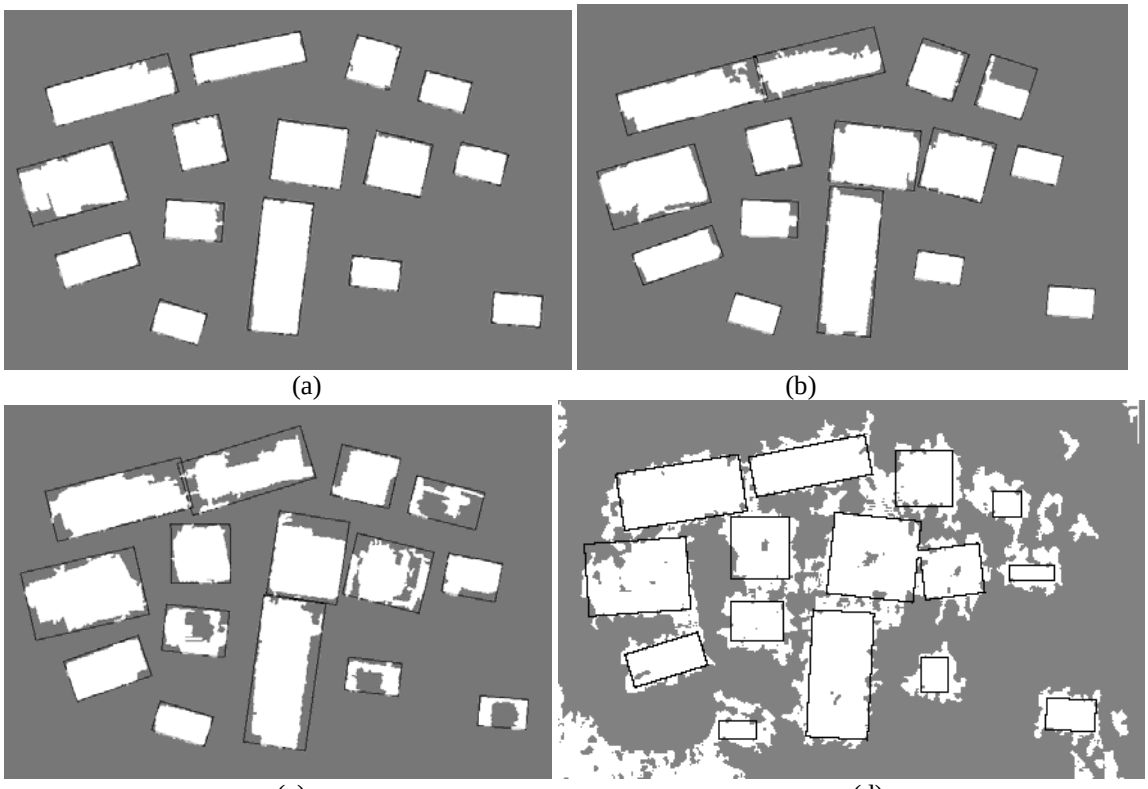

(a) (b)

(c) (d)

Figure 8: Building extraction from simulated interferometric SAR data for the true building height in (a), the building height increased by 15m in (b) and 30m in (c). (d) shows the corresponding result from the real data of Figure 4. White areas correspond to the points selected to be building candidates, the black outlines are the resulting rectangular building models obtained via a minimum bounding rectangle. In (d) the rectangles were calculated after some morphological operations to separate the buildings.

The described approach still works on the simulated height data increased by 15 m in Figure 8b. However, the resulting segmented building areas get larger than the actual buildings due to the "front porch" effect (Bolter 2001). Things are worse for the simulated height data increased by 30 m, some buildings can only be partially recovered (Fig. 8c). Compared with noise-free simulated data, the results are noisier from real data (Fig. 8d). Especially the measured phase noise is transformed to positional displacements in the ground range projected interferometric height data and affects the result.

The area and maximum height inside each segmented building candidate were measured, the results are presented in Table 1.

| | | Simulation | | Real data |
|---|---|---|---|---|
| | True height | Height + 15 m | Height + 30 m | |
| Maximum height | ± 0.15 m | ± 1.2 m | ± 1.9 m | ± 1,0 m[1)] |
| Area | ± 6 m² | ± 41 m² | ± 61 m² | ± 120 m² |

Table 1. Resulting RMS difference between the segmented points in Figure 8 and the corresponding ground truth, using both the simulations and real data. [1)]This error is cleaned of the larger error due to the church steeple.

## 5 ANALYSIS OF SHADOWS

The procedure to extract buildings from the shadows alone operates as follows (Bolter & Leberl 2000b):

Separating shadow pixels with the help of a mask, applied to each image separately;
Morphological operations to find candidate shadows;
Conversion of shadow end points to elevations of vertical objects (building walls);
Merging the independent results from multiple images.

Figure 9 illustrates the result of the shadow operation on simulated and real data. The walls at times seem to indicate the roof shape.

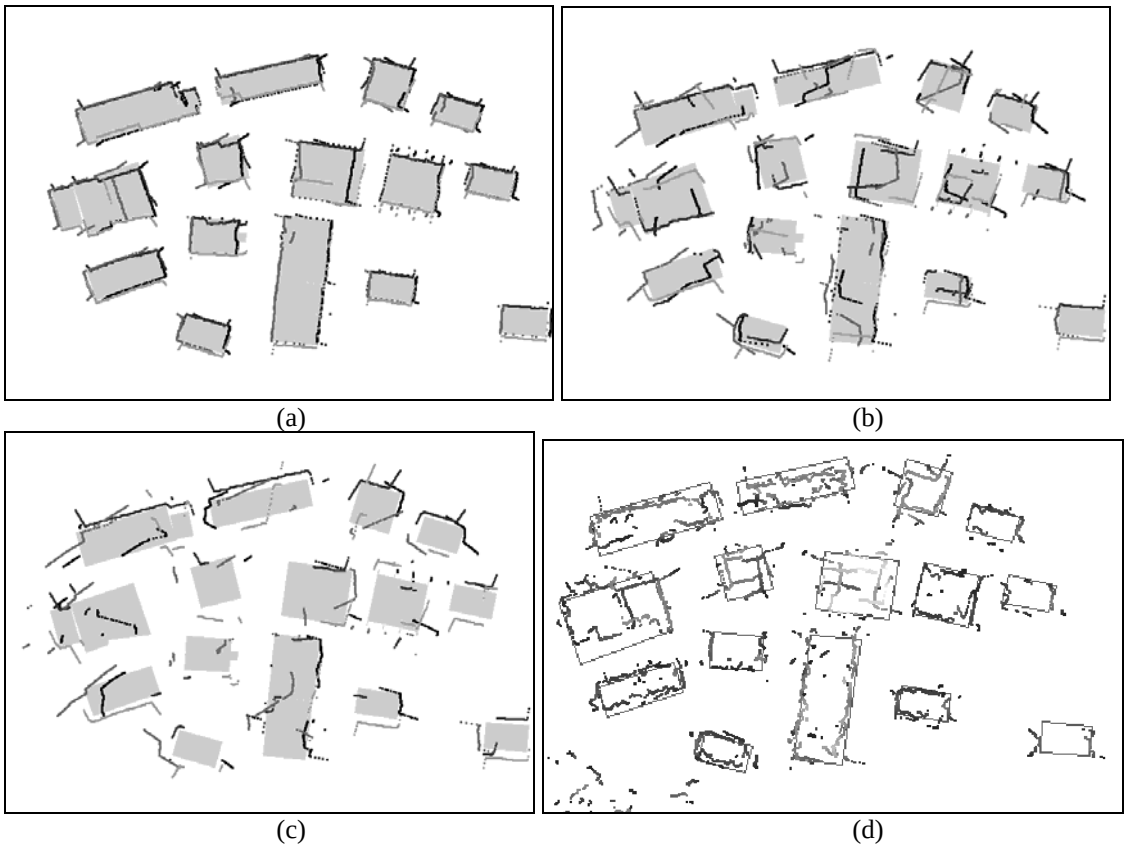


Figure 9: Reconstructed building walls from multiple view shadows for simulated data using the true height (a), increasing the height by 15 m (b) and 30 m (c) and the corresponding result from real data (d). The area covers approximately 220 x 180 m².

The procedure works well on the simulated data using the true height values. From four independent views the outlines of the buildings can be reconstructed. Problems exist if shadow areas are occluded by layover areas of adjacent buildings. Things get worse for increased building heights (Fig. 9b,c), only the outer walls of the building group can be recovered, therefore other strategies have to be found for increasing building heights. The results on the real data (Fig. 9d) on the other hand are useful, the outlines of the buildings can be recovered from the segmented shadows. The elevation errors are at about the same order of magnitude as interferometry, but the footprint area is much improved, from ± 120 m² down to ± 24 m².

## 6 COMBINING SHADOWS AND INTERFEROMETRY

Obviously, the results from interferometry and from shadows differ, especially for real data. It therefore makes sense to look for building shapes that are consistent with both the interferometric as well as the shadow evidence. The approach refines the interferometric building data by means of the shadow analysis. The footprints from the shadows have priority over the footprints from interferometry. The overall accuracy in height does not improve, but the accuracy of the footprints goes from ± 120 $m^2$ to ± 24 $m^2$ (Bolter 2001).

Figure 10 compares the site model recovered automatically from real SAR data with the model of the test site from manual photogrammetry. Simple gable roofed building models were fit to the final point clouds resulting from the combination of interferometry and shadow analysis. Apart from the steeple of the church and the large compund building , where our simple building models are not sufficient to describe the shape, only one building model is obviously wrong. The gable roof of the building indicated by a white ellipse on the upper left of Figure 10 is oriented in the wrong direction.

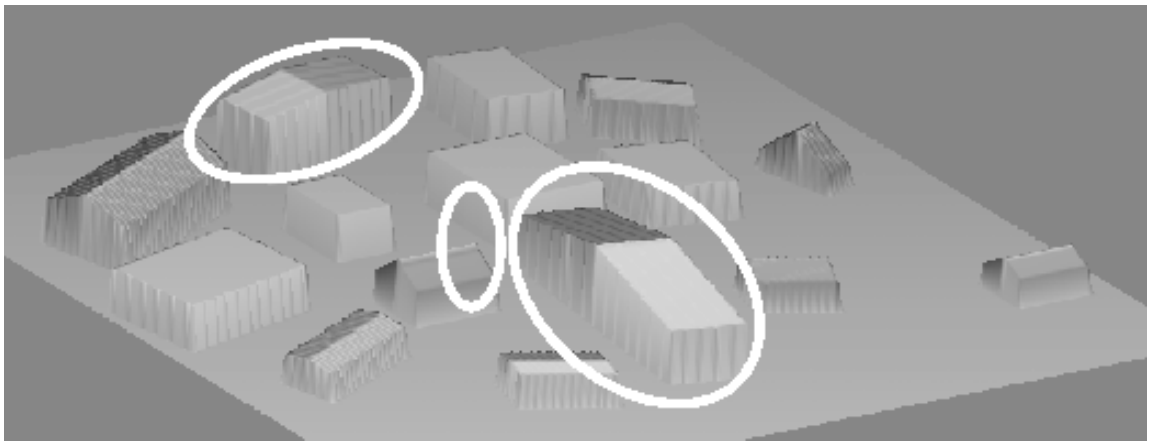

(a)

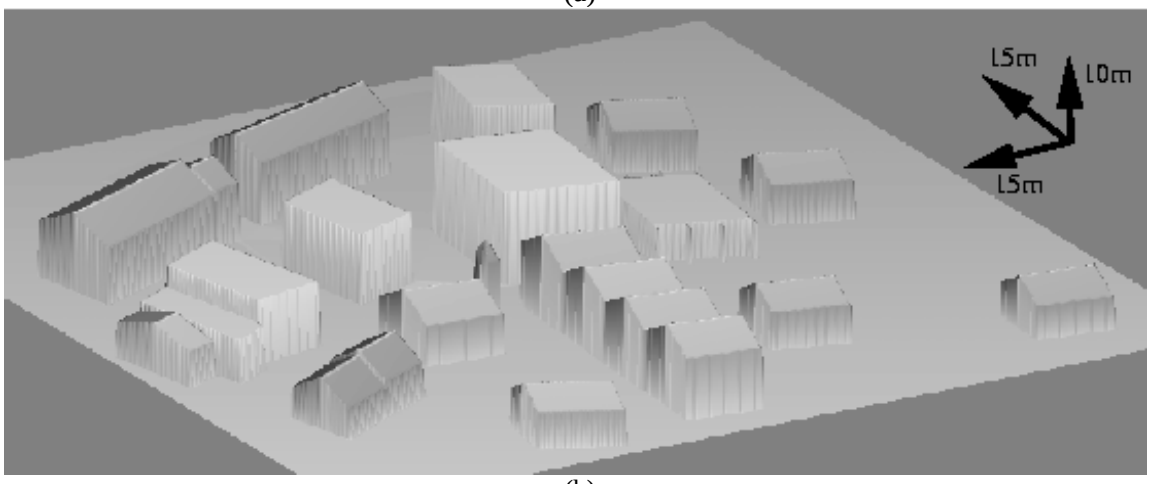


(b)

Figure 10: Shaded view of the SAR site model (a) compared to the ground truth model (b). The area covers approximately 160 x 120 m². The main differences between the two models are indicated by white ellipses in the result from SAR (a). The church steeple was missed, as was the saw-tooth roof because no such shapes were modeled in the approach.

## 7 CONCLUSIONS

We have demonstrated that high resolution SAR grayvalue images and interferometric point clouds are suitable for the creation of 3-dimensional models of buildings. The analysis indicates that an elevation error of about ± 1 m is achievable from source data with a 30 cm pixel diameter. The analysis strategy is applicable to buildings with heights that are smaller than the distance between buildings, in at least one view. The mapping concept is based on multiple flight lines to ensure that various ambiguities due to layovers, front-porch effects and shadow can be resolved. Ongoing work will need to introduce a greater variation in the available pool of test data, and a greater range of procedural alternatives to better respond to a variety of building configurations.

## 8 REFERENCES


Bolter R. 2000. Reconstruction of Man-Made Objects from High Resolution SAR Images. *IEEE Aerospace Conference*, Big Sky, Montana, March 18-25, 2000. ISBN 0-7803-5847-3, CD-ROM, Paper No. 6.0305.

Bolter R. & Leberl F. 2000a. Phenomenology-Based and Interferometry-Guided Building Reconstruction from Multiple SAR Images. *Proceedings of EUSAR 2000*, Munich, pp. 687-690.

Bolter R. & Leberl F. 2000b. Shape-from-Shadow Building Reconstruction from Multiple View SAR Images. In R. Sablatnig, editor, *Applications of 3D-Imaging and Graph-Based Modeling 2000*, 24th Workshop of the Austrian Association for Pattern Recognition (ÖAGM/AAPR), Österreichische Computer Gesellschaft, Band 142, Villach, Austria, May 2000, pp.196-206.

Bolter R. & Leberl F. 2000c. Detection and Reconstruction of Buildings from Multiple View Interferometric SAR Data. *Proceedings of IGARSS 2000*, Hawaii, pp. 749-751.

Bolter R. & Leberl F. 2000d. Detection and Reconstruction of Human Scale Features from High Resolution Interferometric SAR Data. *Proceedings of the ICPR 2000, Volume 4: Applications, Robotics Systems and Architectures*, Barcelona, Spain, pp. 291-294.

Bolter R. & Leberl F. 2000e. Fusion of Multiple View Interferometric and Slant Range SAR Data for Building Reconstruction. EOS/SPIE Remote Sensing Symposium, Barcelona, 2000, *Conference on SAR Image Analysis, Modeling, and Techniques III*, SPIE Vol. 4173, pp. 241-250.

Bolter R. 2001. *Buildings from SAR: Detection and Reconstruction of Buildings from Multiple View High Resolution Interferometric SAR Data*. Dissertation, Graz University of Technology.

Burkhart G., Bergen Z. & Carande R. 1996. Elevation Correction and Building Extraction from Interferometric SAR Imagery, *Proceedings of IGARSS'96*, pp.659-661.

Gamba P., Houshmand B. & Saccani M. 2000. Detection and Extraction of Buildings from Interferometric SAR Data. *IEEE Transactions on Geoscience and Remote Sensing*, 38(1):611-618, January 2000.

Hoepfner K. & Hanson A. & Riseman E. 1998. Recovery of Buildings Structure from SAR and IFSAR Images. In *ARPA Image Understanding Workshop*, pp. 559-563. Morgan-Kaufmann.

Wang Y., Mercer B., Tao V.C., Sharma J. & Crawford S. 2001. Automated Generation of Bald Earth Digital Elevation Models from Digital Surface Models created using Airborne IFSAR. *Proceedings of ASPRS 2001 Gateway to the New Millenium*, April 23-27, St. Louis, Missouri, CD-ROM.

Xiao R., Lesher C. & Wilson B. 1998. Building Detection and Localization using a Fusion of Interferometric Synthetic Aperture Radar and Multispectral Image. *In ARPA Image Understanding Workshop*, pp. 583-588. Morgan Kaufmann.